JACS
JOURNAL OF THE AMERICAN CHEMICAL SOCIETY
Cite This: J. Am. Chem. Soc. 2019, 141, 9788−9792
Communication
pubs.acs.org/JACS

Molecular Ion Fishers as Highly Active and Exceptionally Selective K^+ Transporters

Ruijuan Ye,[†,⊥] Changliang Ren,[‡,⊥] Jie Shen,[‡] Ning Li,[‡] Feng Chen,[‡] Arundhati Roy,[‡] and Huaqiang Zeng*[,‡]

[†]College of Chemistry and Bioengineering, Hunan University of Science and Engineering, Yongzhou, Hunan 425100, China
[‡]The NanoBio Lab, 31 Biopolis Way, The Nanos 138669, Singapore

Supporting Information

ABSTRACT: We report here a unique ion-fishing mechanism as an alternative to conventional carrier or channel mechanisms for mediating highly efficient and exceptionally selective transmembrane K^+ flux. The molecular framework, underlying the fishing mechanism and comprising a fishing rod, a fishing line and a fishing bait/hook, is simple yet modularly modifiable. This feature enables rapid construction of a series of molecular ion fishers with distinctively different ion transport patterns. While more efficient ion transports are generally achieved by using 18-crown-6 as the fishing bait/hook, ion transport selectivity (K^+/Na^+) critically depends on the length of the fishing line, with the most selective **MF6-C14** exhibiting exceptionally high selectivity (K^+/Na^+ = 18) and high activity (EC_{50} = 1.1 mol % relative to lipid).

Artificial molecular machine is a rapidly developing science that often takes a cue from macroscopic objects.[1−11] Recent years have seen a range of fascinating molecular machineries, performing macroscopic functions at the molecular level. Notable examples include molecular muscle,[1] shuttle,[2] switch,[3] rotor,[3,4] propeller,[5] pump,[6] walker,[7] mover,[8] nanocar,[9] synthesizer[10,11] and balance.[12] Awarding of the 2016 Nobel Prize in Chemistry to Jean-Pierre Sauvage,[1] Sir J. Fraser Stoddart[2] and Bernard L. Feringa[3] undoubtedly will catalyze the field to a new height in both fundamental and practical settings.

Although these recent burgeoning scientific advances in molecular machines have greatly increased our ability to manipulate precisely requisite molecular motions and macroscopic functions at the molecular level, researching novel membrane-active molecular machines has lagged far behind. Recently, Zhu and his colleagues reported an interesting example of a rotaxane-derived molecular ion shuttle, nonselectively transporting K^+ ions via a shuttling mechanism with moderate activity (EC_{50} = 3 mol % relative to lipid).[13] We also elaborated a molecular swing mechanism for swinging ions across membrane in a highly efficient but weakly K^+-selective manner.[14] Differing from commonly seen carrier[15−19] and channel[20−31] mechanisms, these alternative ion-shuttling and -swinging mechanisms[13,14] suggest that unconventional ion transport mechanisms could also work properly in a membrane environment.

Herein, we disclose another unconventional ion-fishing mechanism for delivering highly active and exceptionally selective transport of K^+ ions. Despite their simple structure and easey synthesis, a number of these ion fishers are highly K^+-selective, with the most selective **MF6-C14** transporting K^+ ions three times as fast as the complex and nonselective rotaxane-based ion shuttle,[13] and with an exceptional K^+/Na^+ selectivity of 18—seven times that of the molecular swing (K^+/Na^+ = 2.4).[14] These ion fishers therefore are among the most selective K^+ transporters.[32−36] In fact, the highest unambiguously determined K^+/Na^+ selectivity of 9.8 was achieved only in 2017 through a combinatorial screening.[37]

We have a long interest in developing novel membrane-active transporters.[14,37−40] Inspired by the popular angling fishing method where recreational fishers use a combination of fishing tackles to catch fish, we designed a series of molecular ion fishers (**MF**s), performing a catch-and-release ion-fishing function within the context of lipid membrane. Structurewise, we covalently integrate three essential and modularly tunable types of fishing tackles (e.g., fishing rod, fishing line and fishing bait/hook) with appropriate dimensions into nanometer-sized **MF**s. The combined hydrophobic length (30−36 Å, Figure 1a) matches a typical hydrophobic membrane thickness (34 Å). Serving as the lipid anchor to firmly anchor the **MF**s into one side of the membrane region, the hydroxyl-rich cholesterol group with a rigid and linear backbone also functions as a rigid fishing rod to orient both the flexible alkyl chain-based fishing ropes of 21−27 Å and a crown ether-based fishing bait/hook mostly in parallel with the hydrophobic lipid tails. Energetically, the computationally optimized linear conformation is at its thermodynamically most stable state (see **MF5-C10**, Figure 1b).

Apparently, the catch-and-release fishing activity should take place in four sequential steps (Figure 1c). First, the **MF** in a fully extended state catches an ion through its fishing bait/hook from one side of the membrane. Driven by an ion concentration gradient, it curls up to allow the ion to cross the central line of the hydrophobic membrane region in step 2. After some further upward movement toward the membrane−water interface, it releases the ion to the other side of the membrane in step 3, and returns to its most stable extended state in step 4 to start another ion-fishing cycle. Since the ion

Received: April 22, 2019
Published: June 11, 2019

DOI: 10.1021/jacs.9b04096
J. Am. Chem. Soc. 2019, 141, 9788−9792

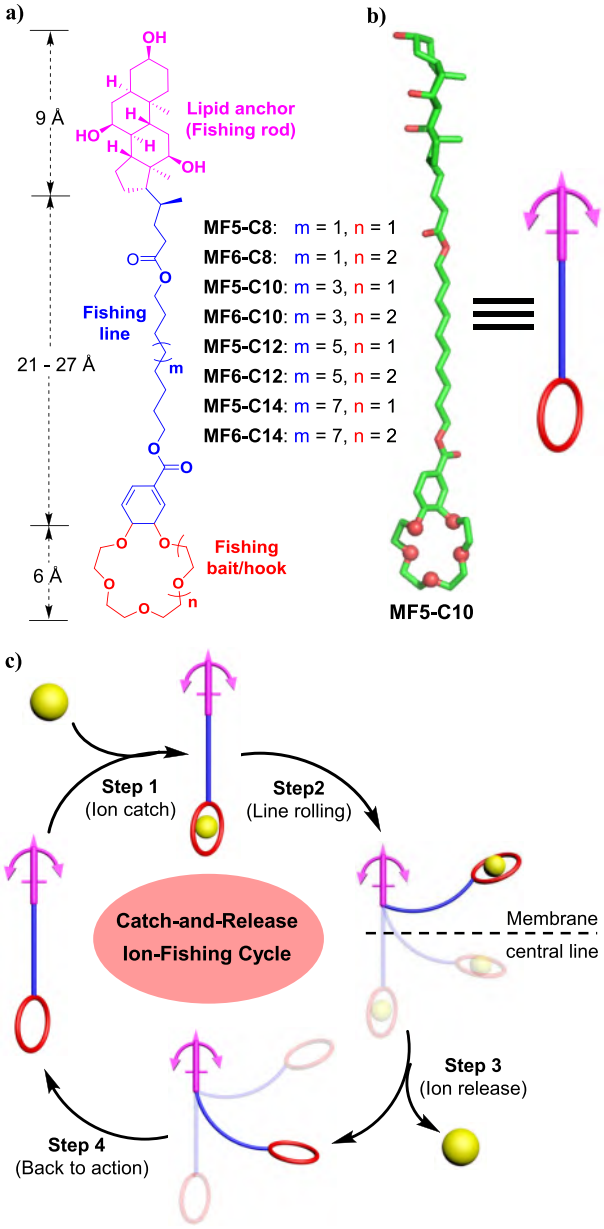

Figure 1. (a) Molecular design of ion fishers **MF5**s and **MF6**s. (b) Computationally optimized structure of **MF5-C10** at the B3LYP/6-31G* level. (c) Proposed catch-and-release ion-fishing mechanism for fishing ions across membrane.

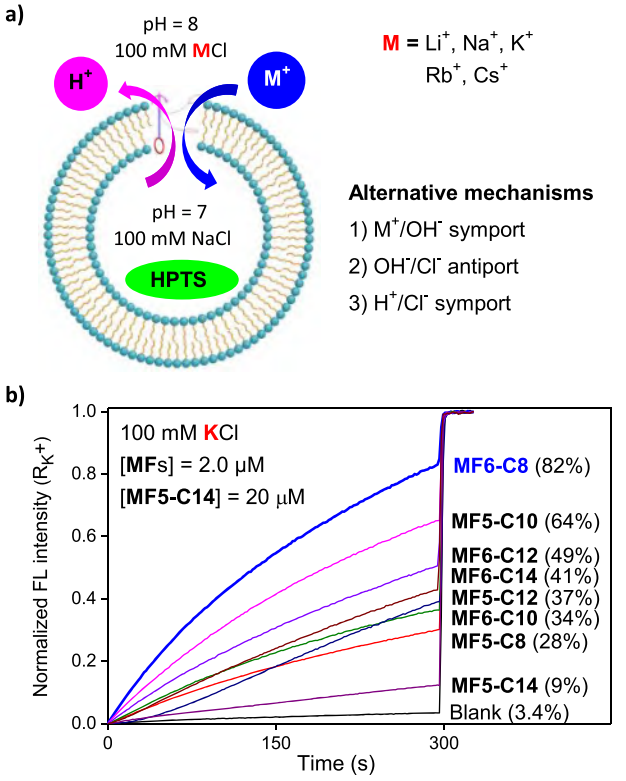

Figure 2. (a) pH-sensitive HPTS assay for ion transport study. (b) K^+ transport curves for various **MF**s. $R_K^+ = (I_K^+ - I_0)/(I_{Triton} - I_0)$.

experiences the most pronounced energetic penalty in the center of the hydrophobic membrane region, the ability of **MF**s to overcome such resistance and bring the ion to cross the membrane central line determines whether the proposed fishing mechanism could work in lipid membrane or not and the ion-fishing efficiency.

To examine the applicability and efficacy of the hypothetic ion-fishing mechanism, we designed two sets of **MF**s, containing 15-crown-5 (**MF5**) or 18-crown-6 (**MF6**) units as the fishing bait/hook, respectively, with the fishing line tuned from C_8H_{16} to $C_{14}H_{28}$. Using the pH-sensitive 8-hydroxypyrene-1,3,6-trisulfonic acid (HPTS) assay (Figure 2a), K^+ ions are found to transport faster than Na^+ ions by most **MF**s, with **MF6-C8** displaying the highest transport activity (Figure 2b). While **MF6-C8** at 2.5 μM and **MF6-C14** at 10 μM achieve R_K^+ values of >93%, the R_K^+ values of <6% for all control compounds (**FR-C8**, **FR-C10**, **C5** and **C6**, Figure S1c) at 10 μM are comparable to the background signal (3.4%).

The Hill analyses were conducted to determine EC_{50} values for Na^+ and K^+ ions (Figures S2–S5 and Table 1). Six out of eight **MF**s are found to be K^+-selective. **MF5-C10**, **MF6-C8**, **MF6-C12** and **MF6-C14** exhibit both high activity (EC_{50} = 0.81–2.7 μM = 0.37–1.2 mol % relative to lipid) and high selectivity (K^+/Na^+ > 7), and **MF5-C12** and **MF5-C14** are weakly active but Na^+-selective.

Although the ratio of EC_{50} values is a widely used parameter for comparing ion transport selectivity, they might not be sufficiently accurate when transporters (1) have a poor solubility, (2) experience self-aggregation or unfavorable interactions with lipids or (3) form a multimolecular channel whose active components do not increase proportionally with the increased concentrations. For instance, **MF6-C12**, requiring an unobstructed large space for proper function via an ion-fishing mechanism, may find a surrounding environment overcrowded at high concentrations. That is, are these two ion fishers, having high K^+/Na^+ selectivity of >28 estimated from the EC_{50} values, truly so K^+-selective?

To alleviate these possible issues, we previously used highly K^+-selective **5F8** (Figure S6) as the reference channel and proposed the use of ratio of R_K^+/R_{Na}^+ as a complementary and reliable index for selectivity assessment.[37] In our previous work, **5F8** was unambiguously determined to have K^+/Na^+ selectivity of 9.8 using single-channel current measurements, with ratios of 4.5 and 14.7 for EC_{50} (Na^+)/EC_{50} (K^+) and R_K^+/R_{Na}^+, respectively.

In this work, we found that a membrane dialysis method, rather than flash column chromatography, to separate the excessive unencapsulated HPTS from large unilamellar lip-

DOI: 10.1021/jacs.9b04096
J. Am. Chem. Soc. 2019, 141, 9788–9792

Table 1. Determined values for EC_{50} (μM), EC_{50} (Na^+)/EC_{50} (K^+) and $R_K{}^+/R_{Na}{}^+$

	MF5-C8	MF5-C10	MF5-C12	MF5-C14	MF6-C8	MF6-C10	MF6-C12	MF6-C14
EC_{50} (Na^+) [a]	5.1 ± 0.2	10.1 ± 0.2	30.9 ± 2.9	55.9 ± 1.7	10.1 ± 0.8	4.6 ± 0.2	49.2 ± 3.4	>> 70
EC_{50} (K^+) [a]	4.6 ± 0.3	1.4 ± 0.1	>> 30	>> 70	0.81 ± 0.1	2.7 ± 0.1	1.7 ± 0.1	2.5 ± 0.1
$\frac{EC_{50}(Na^+)}{EC_{50}(K^+)}$	1.1	7.2	< 1	< 1	12.5	1.7	28.9	> 28
$R_K{}^+/R_{Na}{}^+$ [b]	1.1	5.2	1.8	0.3	7.1	1.4	7.8	18.0

[a][Total lipid] = 219 μM. [b]See Figure S9 for more detail.

osomes (LUVs) consistently produces LUVs that exhibit low background signals of 3−8% (Figure S7). Using these tight LUVs, the EC_{50} (K^+) of **5F8** was redetermined to be 5.2 μM (Figure S6), which is similar to previously determined 5.5 μM.[37] Importantly, at [**5F8**] = 11 μM where **5F8** elicits a $R_K{}^+$ value of 92.3%, $R_K{}^+/R_{Na}{}^+$ was determined to be 9.6 (Figure S8), which is nearly identical to the absolute K^+/Na^+ selectivity of 9.8. This suggests ratios of $R_K{}^+/R_{Na}{}^+$ determined using LUVs with low background signals allows ion selectivity to be gauged reliably even though it still may differ from the true ion selectivity.

To obtain meaningful $R_M{}^+$ values ($R_K{}^+$, $R_{Na}{}^+$, etc.) and ratio **R** (e.g., $R_K{}^+/R_{Na}{}^+$) for a reliable comparison of ion selectivity, it is imperative to determine $R_M{}^+$ at the concentration where the channel's transport activity has been maximized to >90% or reached saturation over 300 s for the most active ion (Figures 3a and S9). Following this criterion, we have obtained all $R_M{}^+$ values (M = Li^+, Na^+, K^+, Rb^+ and Cs^+) for all eight **MF**s (Figure S9), with ratios of $R_K{}^+/R_{Na}{}^+$ presented in Table 1.

As evidenced from $R_M{}^+$ and ratio **R** values, seven out of eight **MF**s are K^+-selective, including **MF5-C12** otherwise shown to be Na^+-selective using EC_{50} values. The most K^+-selective **MF6-C14** displays exceptional K^+/Na^+ selectivity of 18 (Figure 3a), yet with high activity (EC_{50} = 2.5 μM or 1.1 mol % relative to lipid). **MF6-C8** (EC_{50} = 0.81 μM) and **MF6-C12** (EC_{50} = 1.7 μM) also display high K^+/Na^+ selectivities of 7.1 and 7.8, respectively.

Interestingly, although **MF5-C14** is weakly active, it displays good Na^+/K^+ selectivity of 3.6 and high selectivity against Rb^+ (Na^+/Rb^+ = 21) and Cs^+ (Na^+/Cs^+ = 65). More interestingly, all eight **MF**s do not transport Li^+ ions (Figure S9). This consistent observation is in sharp contrast to our best knowledge that all crown ether-based ion channels with ion transport activities tested against Li^+ ions transport Li^+ ions. This may imply that the large dehydration energy of Li^+ ions cannot be compensated for by the crown ether unit that functions through a fishing mechanism, but likely can be sufficiently compensated for by a channel mechanism.

The M^+ ions as the main transport species were established by the chloride-sensitive 6-methoxy-*N*-(3-sulfopropyl)-quinolinium (SPQ) assay (Figure 3b). Compared to anion channel **L8**[39] that causes 65% fluorescence quenching of SPQ dye at 3 μM, that no significant fluorescence quenching by both **MF6-C8** and **MF6-C14** was observed signifies the inability of **MF**s to transport anions.

The transport rates between K^+ and H^+ were compared using a proton carrier **FCCP** (Figure 3c). With respect to no change in fluorescence intensity between FCCP alone and the background signal, a net increase of 44% between transport

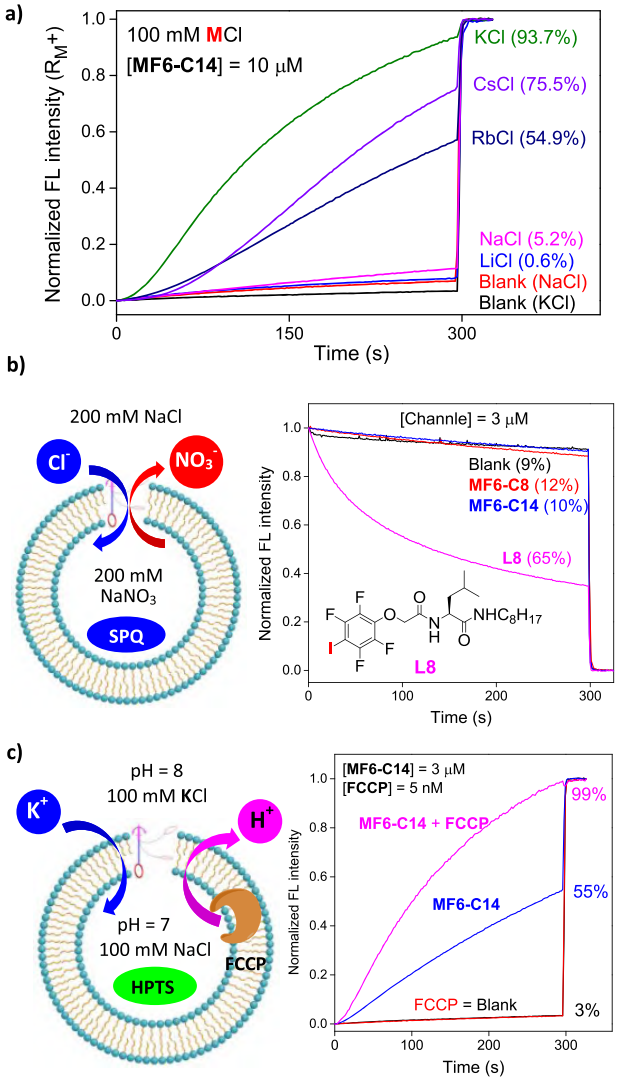

Figure 3. (a) Ion transport percentages ($R_M{}^+$) for **MF6-C14** at 10 μM. (b) SPQ assay to confirm the inability of **MF**s to transport anions. (c) FCCP-based HPTS assay to confirm that **MF6-C14** transports K^+ ions faster than H^+ ions.

activities mediated by **MF6-C14** in the absence (55%) and presence (99%) of **FCCP** suggests K^+ to be transported much faster than H^+. A similar conclusion can be drawn for **MF6-C8** (Figure S10).

The carboxyfluorescein-leakage assay (λ_{ex} = 492 nm, λ_{em} = 517 nm, Figure S11) shows that melittin, which forms a pore of >1 nm or efficiently lysates the membrane at low

DOI: 10.1021/jacs.9b04096
J. Am. Chem. Soc. 2019, 141, 9788−9792

concentrations, results in large increases in fluorescence by 54% and 86% at 100 and 200 nM, respectively. In contrast, both **MF6-C8** and **MF6-C14** produce changes of <2% at 5 μM. These results support well-maintained membrane integrity in the presence of **MF**s, ruling out the membrane-lysing activity of **MF**s.

Additional structure−activity-relationship studies on shorter **MF6-C2**, **MF6-C4** and **MF6-C6** (Figures 4 and S12−S14) reveal that the K^+ transport activity peaks at **MF6-C8** (EC_{50} = 0.81 μM), with the highest K^+/Na^+ selectivity achieved by **MF6-C14**.

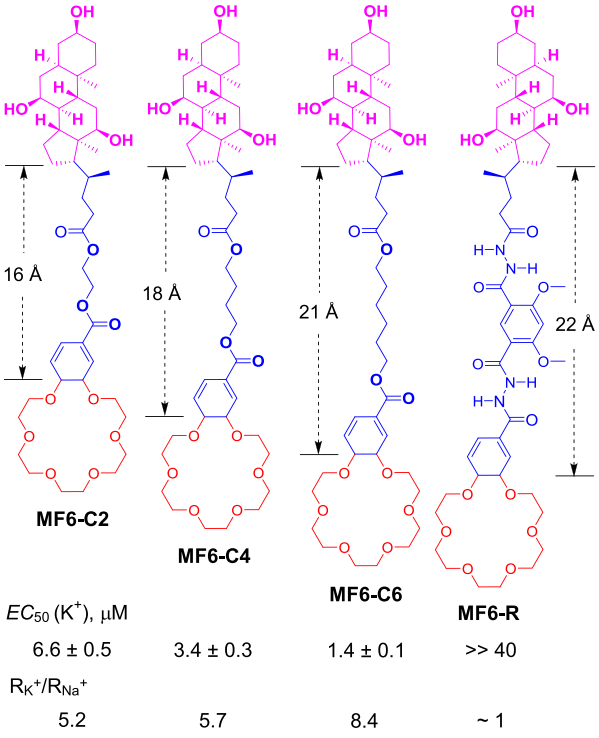

Figure 4. Structures and ion transport properties of the shorter (**MF6-C2**, **MF6-C4** and **MF6-C6**) and more rigid (**MF6-R**) **MF**s.

Further, from the stepwise analyses of the catch-and-release ion-fishing cycle (Figure 1c), this ion-fishing mechanism shares some similarity with but also differs from carrier and channel mechanisms. Like carriers, **MF**s are not simultaneously open to both the intra- and extra-cellular environments. Like channels, they do follow a defined pathway with one end fixed in the lipid membrane through the cholesterol unit to facilitate ion transport via a fishing mechanism. To examine to which of the two mechanisms the ion-fishing mechanism is closer, we conducted single-channel current measurements on **MF6-C14**. The fact that our extensive efforts failed to record single-channel current traces suggests these ion fishers likely operate in a carrier-like mechanism.

Lastly, unlike the conventional ion carriers that can move freely and randomly in both vertical and lateral directions, the **MF**s can only move the same way laterally. More specifically, the rigid cholesterol backbone, which acts as the lipid anchor, cannot move vertically, with the remaining flexible part freely curling up or down in a manner akin to a fishing process. Consequently, one expects to see greatly diminished ion-fishing activity upon replacing the flexible fishing rope with a rigid one that cannot bend. We therefore prepared **MF6-R** rigidified by intramolecular H-bonds (Figure 4). Consistent with the proposed ion-fishing mechanism, **MF6-R** indeed exhibits extremely weak activities ($EC_{50} \gg 40$ μM) for both K^+ and Na^+ ions (Figure S13b).

In summary, we have established here a novel "catch-and-release ion-fishing" strategy for achieving highly efficient and remarkably selective transport of K^+ ions across membrane. It is also of exceptional interest to note that all ion fishers studied herein do not transport Li^+ ions, a feature that is unprecedented among ion channels derived from crown ethers. Further, it is postulated that this class of ion fishers does not have a single ion permeation pathway to follow. Rather, while operating in a more carrier-like mechanism, they fish ions through numerous pathways that are more defined than carriers but less defined than channels. Given their highly modular nature and easy synthesis, a broad range of molecular ion fishers can be readily envisioned, possibly exhibiting outstanding membrane transport properties for promising medical applications.

■ ASSOCIATED CONTENT

Supporting Information

The Supporting Information is available free of charge on the ACS Publications website at DOI: 10.1021/jacs.9b04096.

Synthetic procedures and a full set of characterization data including ^{1}H NMR, ^{13}C NMR and MS as well as a complete set of ion transport study (PDF)

■ AUTHOR INFORMATION

Corresponding Author

*hqzeng@nbl.a-star.edu.sg

Author Contributions

⊥R.Y. and C.R. contributed equally to the work.

Notes

The authors declare no competing financial interest.

■ ACKNOWLEDGMENTS

This work was supported by the NanoBio Lab (Biomedical Research Council, Agency for Science, Technology and Research, Singapore) and the construct program of applied characteristic discipline in Hunan University of Science and Engineering

■ REFERENCES

(1) Sauvage, J.-P. From Chemical Topology to Molecular Machines (Nobel Lecture). *Angew. Chem., Int. Ed.* **2017**, *56*, 11080−11093.

(2) Stoddart, J. F. Mechanically Interlocked Molecules (MIMs)—Molecular Shuttles, Switches, and Machines (Nobel Lecture). *Angew. Chem., Int. Ed.* **2017**, *56*, 11094−11125.

(3) Feringa, B. L. The Art of Building Small: From Molecular Switches to Motors (Nobel Lecture). *Angew. Chem., Int. Ed.* **2017**, *56*, 11060−11078.

(4) Erbas-Cakmak, S.; Fielden, S. D. P.; Karaca, U.; Leigh, D. A.; McTernan, C. T.; Tetlow, D. J.; Wilson, M. R. Rotary and linear molecular motors driven by pulses of a chemical fuel. *Science* **2017**, *358*, 340−343.

(5) Simpson, C. D.; Mattersteig, G.; Martin, K.; Gherghel, L.; Bauer, R. E.; Räder, H. J.; Müllen, K. Nanosized Molecular Propellers by Cyclodehydrogenation of Polyphenylene Dendrimers. *J. Am. Chem. Soc.* **2004**, *126*, 3139−3147.

(6) Cheng, C.; McGonigal, P. R.; Schneebeli, S. T.; Li, H.; Vermeulen, N. A.; Ke, C.; Stoddart, J. F. An artificial molecular pump. *Nat. Nanotechnol.* **2015**, *10*, 547−553.

DOI: 10.1021/jacs.9b04096
J. Am. Chem. Soc. 2019, 141, 9788−9792

(7) von Delius, M.; Geertsema, E. M.; Leigh, D. A. A synthetic small molecule that can walk down a track. *Nat. Chem.* **2010**, *2*, 96−101.
(8) Kassem, S.; Lee, A. T. L.; Leigh, D. A.; Markevicius, A.; Solà, J. Pick-up, transport and release of a molecular cargo using a small-molecule robotic arm. *Nat. Chem.* **2016**, *8*, 138−143.
(9) Kudernac, T.; Ruangsupapichat, N.; Parschau, M.; Maciá, B.; Katsonis, N.; Harutyunyan, S. R.; Ernst, K.-H.; Feringa, B. L. Electrically driven directional motion of a four-wheeled molecule on a metal surface. *Nature* **2011**, *479*, 208−211.
(10) Lewandowski, B.; De Bo, G.; Ward, J. W.; Papmeyer, M.; Kuschel, S.; Aldegunde, M. J.; Gramlich, P. M. E.; Heckmann, D.; Goldup, S. M.; D'Souza, D. M.; Fernandes, A. E.; Leigh, D. A. Sequence-Specific Peptide Synthesis by an Artificial Small-Molecule Machine. *Science* **2013**, *339*, 189−193.
(11) Thordarson, P.; Bijsterveld, E. J. A.; Rowan, A. E.; Nolte, R. J. M. Epoxidation of polybutadiene by a topologically linked catalyst. *Nature* **2003**, *424*, 915−918.
(12) Paliwal, S.; Geib, S.; Wilcox, C. S. Molecular Torsion Balance for Weak Molecular Recognition Forces. Effects of "Tilted-T" Edge-to-Face Aromatic Interactions on Conformational Selection and Solid-State Structure. *J. Am. Chem. Soc.* **1994**, *116*, 4497−4498.
(13) Chen, S.; Wang, Y.; Nie, T.; Bao, C.; Wang, C.; Xu, T.; Lin, Q.; Qu, D.-H.; Gong, X.; Yang, Y.; Zhu, L.; Tian, H. An Artificial Molecular Shuttle Operates in Lipid Bilayers for Ion Transport. *J. Am. Chem. Soc.* **2018**, *140*, 17992−17998.
(14) Ren, C. L.; Chen, F.; Ye, R. J.; Ong, Y. S.; Lu, H. F.; Lee, S. S.; Ying, J. Y.-R.; Zeng, H. Q. Molecular swings as highly active ion transporters. *Angew. Chem., Int. Ed.* **2019**, *58*, 8034−8038.
(15) Davis, J. T.; Okunola, O.; Quesada, R. Recent advances in the transmembrane transport of anions. *Chem. Soc. Rev.* **2010**, *39*, 3843−3862.
(16) Brotherhood, P. R.; Davis, A. P. Steroid-based anion receptors and transporters. *Chem. Soc. Rev.* **2010**, *39*, 3633−3647.
(17) Kim, D. S.; Sessler, J. L. Calix[4]pyrroles: versatile molecular containers with ion transport, recognition, and molecular switching functions. *Chem. Soc. Rev.* **2015**, *44*, 532−546.
(18) Benz, S.; Macchione, M.; Verolet, Q.; Mareda, J.; Sakai, N.; Matile, S. Anion Transport with Chalcogen Bonds. *J. Am. Chem. Soc.* **2016**, *138*, 9093−9096.
(19) Gale, P. A.; Davis, J. T.; Quesada, R. Anion transport and supramolecular medicinal chemistry. *Chem. Soc. Rev.* **2017**, *46*, 2497−2519.
(20) Gokel, G. W.; Murillo, O. Synthetic Organic Chemical Models for Transmembrane Channels. *Acc. Chem. Res.* **1996**, *29*, 425−432.
(21) Matile, S.; Vargas Jentzsch, A.; Montenegro, J.; Fin, A. Recent synthetic transport systems. *Chem. Soc. Rev.* **2011**, *40*, 2453−2474.
(22) Vargas Jentzsch, A.; Hennig, A.; Mareda, J.; Matile, S. Synthetic Ion Transporters that Work with Anion−π Interactions, Halogen Bonds, and Anion−Macrodipole Interactions. *Acc. Chem. Res.* **2013**, *46*, 2791−2800.
(23) Montenegro, J.; Ghadiri, M. R.; Granja, J. R. Ion Channel Models Based on Self-Assembling Cyclic Peptide Nanotubes. *Acc. Chem. Res.* **2013**, *46*, 2955−2965.
(24) Fyles, T. M. How Do Amphiphiles Form Ion-Conducting Channels in Membranes? Lessons from Linear Oligoesters. *Acc. Chem. Res.* **2013**, *46*, 2847−2855.
(25) Otis, F.; Auger, M.; Voyer, N. Exploiting Peptide Nanostructures To Construct Functional Artificial Ion Channels. *Acc. Chem. Res.* **2013**, *46*, 2934−2943.
(26) Gokel, G. W.; Negin, S. Synthetic Ion Channels: From Pores to Biological Applications. *Acc. Chem. Res.* **2013**, *46*, 2824−2833.
(27) Barboiu, M.; Gilles, A. From Natural to Bioassisted and Biomimetic Artificial Water Channel Systems. *Acc. Chem. Res.* **2013**, *46*, 2814−2823.
(28) Gong, B.; Shao, Z. Self-Assembling Organic Nanotubes with Precisely Defined, Sub-nanometer Pores: Formation and Mass Transport Characteristics. *Acc. Chem. Res.* **2013**, *46*, 2856−2866.
(29) Si, W.; Xin, P.; Li, Z.-T.; Hou, J.-L. Tubular Unimolecular Transmembrane Channels: Construction Strategy and Transport Activities. *Acc. Chem. Res.* **2015**, *48*, 1612−1619.
(30) Huo, Y. P.; Zeng, H. Q. Sticky"-Ends-Guided Creation of Functional Hollow Nanopores for Guest Encapsulation and Water Transport. *Acc. Chem. Res.* **2016**, *49*, 922−930.
(31) Chen, J.-Y.; Hou, J.-L. Controllable synthetic ion channels. *Org. Chem. Front.* **2018**, *5*, 1728−1736.
(32) Xin, P.; Zhu, P.; Su, P.; Hou, J.-L.; Li, Z.-T. Hydrogen-Bonded Helical Hydrazide Oligomers and Polymer That Mimic the Ion Transport of Gramicidin A. *J. Am. Chem. Soc.* **2014**, *136*, 13078−13081.
(33) Gilles, A.; Barboiu, M. Highly Selective Artificial K+ Channels: An Example of Selectivity-Induced Transmembrane Potential. *J. Am. Chem. Soc.* **2016**, *138*, 426−432.
(34) Lang, C.; Deng, X.; Yang, F.; Yang, B.; Wang, W.; Qi, S.; Zhang, X.; Zhang, C.; Dong, Z.; Liu, J. Highly Selective Artificial Potassium Ion Channels Constructed from Pore-Containing Helical Oligomers. *Angew. Chem.* **2017**, *129*, 12842−12845.
(35) Sun, Z.; Barboiu, M.; Legrand, Y.-M.; Petit, E.; Rotaru, A. Highly Selective Artificial Cholesteryl Crown Ether K+-Channels. *Angew. Chem.* **2015**, *127*, 14681−14685.
(36) Xin, P.; Kong, H.; Sun, Y.; Zhao, L.; Fang, H.; Zhu, H.; Jiang, T.; Guo, J.; Zhang, Q.; Dong, W.; Chen, C.-P. Artificial K+ Channels Formed by Pillararene-Cyclodextrin Hybrid Molecules: Tuning Cation Selectivity and Generating Membrane Potential. *Angew. Chem., Int. Ed.* **2019**, *58*, 2779−2784.
(37) Ren, C. L.; Shen, J.; Zeng, H. Q. Combinatorial evolution of fast-conducting highly selective K+-channels via modularly tunable directional assembly of crown ethers. *J. Am. Chem. Soc.* **2017**, *139*, 12338−12341.
(38) Zhao, H. Q.; Sheng, S.; Hong, Y. H.; Zeng, H. Q. Proton Gradient-Induced Water Transport Mediated by Water Wires inside Narrow Aquapores of Aquafoldamer Molecules. *J. Am. Chem. Soc.* **2014**, *136*, 14270−14276.
(39) Ren, C. L.; Ding, X.; Roy, A.; Shen, J.; Zhou, S.; Chen, F.; Yau Li, S. F.; Ren, H.; Yang, Y. Y.; Zeng, H. Q. A halogen bond-mediated highly active artificial chloride channel with high anticancer activity. *Chem. Sci.* **2018**, *9*, 4044−4051.
(40) Ren, C. L.; Zeng, F.; Shen, J.; Chen, F.; Roy, A.; Zhou, S.; Ren, H.; Zeng, H. Q. Pore-Forming Monopeptides as Exceptionally Active Anion Channels. *J. Am. Chem. Soc.* **2018**, *140*, 8817−8826.

DOI: 10.1021/jacs.9b04096
J. Am. Chem. Soc. 2019, 141, 9788−9792